https://doi.org/10.15407/ujpe69.10.742

A. JUMABAEV,[1] H. HUSHVAKTOV,[1] A. ABSANOV,[1] B. KHUDAYKULOV,[1]
Z. ERNAZAROV,[1] L. BULAVIN[2]

[1] Sharof Rashidov Samarkand State University
(15, University Blvd., Samarkand 703004, Uzbekistan; e-mail: abduvakhidj@gmail.com)
[2] Taras Shevchenko National University of Kyiv
(64/13, Volodymyrska Str., Kyiv 01601, Ukraine)

VIBRATIONAL SPECTRA AND COMPUTATIONAL STUDY OF AMYL ACETATE: MEP, AIM, RDG, NCI, ELF AND LOL ANALYSIS

This work is focused on biologically active neat amyl acetate and its solutions in ethanol/heptane. According to the experimental results, when the concentration of amyl acetate in the amyl acetate-ethanol solution decreases, the additional band appears on the low-frequency side. The primary reason for the formation of such additional band is the intermolecular hydrogen bonding between amyl acetate and ethanol. In the amyl acetate-heptane solution, as the concentration of amyl acetate in the solution decreases, the band corresponding to the C=O stretching vibrations shifted to a higher frequency. This is explained by the fact that heptane breaks intermolecular interactions in solution, resulting in a simpler spectral band corresponding to the C=O stretching vibrations. Calculations are also used to study interactions in amyl acetate-ethanol complexes and their spectral manifestations. When the complex formation energies are calculated, this energy increases with the number of molecules, but the average hydrogen bond energy per one bond remains unchanged. The density functional theory (DFT) method is used to analyze molecular structural parameters: Mulliken atomic charge distribution; thermodynamic parameters; molecular electrostatic potential (MEP) surface; atoms in molecules (AIM) analysis; quantum chemical parameters such as reduced density gradient (RDG) and noncovalent interaction (NCI) analysis; electron localization functions (ELF) analysis; and localized orbital locator (LOL) analysis.

Keywords: Raman spectroscopy, quantum chemical calculations, DFT, hydrogen bonding, molecular electrostatic potential, electron localization function, localized orbital locator, RDG diagram, Mulliken charge distribution, amyl acetate, ethanol, heptane.

1. Introduction

Studying the nature and dynamics of intermolecular interactions is important in chemistry, biology and materials science [1–7]. Understanding the liquid structure and intermolecular interactions in the liquid phase is essential for the microscopic investigation of the solution formation [8]. A hydrogen bond, represented as X–H...Y [9, 10], exists between a proton donor (Y) and a proton acceptor. According to Pauling's definition, both X and Y are electronegative atoms (for example, O and N) [11]. After the formation of a complex through H-bonding, the X-H bond length changes due to the electron transfer to X–H [12, 13]. Such an electronic transition increases the

Citation: Jumabaev A., Hushvaktov H., Absanov A., Khudaykulov B., Ernazarov Z., Bulavin L. Vibrational spectra and computational study of amyl acetate: MEP, AIM, RDG, NCI, ELF and LOL analysis. *Ukr. J. Phys.* **69**, No. 10, 742 (2024). https://doi.org/10.15407/ujpe69.10.742.
© Publisher PH "Akademperiodyka" of the NAS of Ukraine, 2024. This is an open access article under the CC BY-NC-ND license (https://creativecommons.org/licenses/by-nc-nd/4.0/)

length of the X-H bond, while shifting its vibrational frequency to lower frequencies [14, 15]. Non-classical hydrogen bonds are formed via aliphatic ethers with hydrogen (H)-bond donors (C–H) and acceptors (carbonyl and ester oxygen) [9]. One of these esters is amyl acetate, which is biologically active. The substance has widespread application in the pharmaceutical, chemical, and biological industries [16]. It also plays a role in the extraction of vegetable oil [16–18], paints, adhesives, plastics, the petrochemical sector, polymers, and the manufacture of circuits for electronics [19, 20].

Mahendraprabu *et al.* analyzed the hydrogen bonds between ethyl acetate and methylcellulose, one of the aliphatic ethers, by FTIR and dielectric methods [21]. C–H...O and O–H...O bonds were identified. Double frequency of hydrogen bond (C=O) was observed in methylcellulose. In that work, CH_3 symmetric and asymmetric, C=O, C–C–O and O–CH_2–C streetching vibration frequencies were analyzed [21]. The C=O group is an ideal representative in the investigation of proteins, and the C=O streetching vibrational frequency is observed around 1700 cm^{-1} [22, 23]. In aliphatic ethers, it was noticed that the C=O streetching vibration band corresponds to the interval 1735–1750 cm^{-1} [24]. In addition, when aliphatic ethers are dissolved in polar and non-polar solvents, this band shifts down [25]. Moreover, a new band can be formed on the low-frequency side. In this case, when dissolved in a solvent, the complex has an open-type geometry, and two C=O vibration bands appear. One of them is caused by the streetching vibrations of the hydrogen-bonded carbonyl group, and the other one is caused by the breaking of the H-bond. Thus, the presence of an open dimer along with a monomer in aliphatic ethers leads to the formation of three carbonyl streetching bands. Therefore, it can be seen that the C=O vibrational frequency splits into two ones. One of them is related to symmetrical monomers, and the other one is related to closed dimers formed by the solution [26].

According to the above literature review, a change in the spectral band shape of amyl acetate in various solutions has not been completed as of this point, and requiring scientific investigation in this area. The main goal of this work is to investigate the solutions of amyl acetate with ethanol and heptane using experimental and quantum-chemical calculations. In addition, various topological: structural parameters of molecules; Mulliken atomic charge distribution; thermodynamic parameters; MEP surface; AIM; RDG; such as NCI; ELF; and LOL analyses were performed using the DFT method.

2. Experimental Method

The Raman spectrum of neat and ethanol/heptane solutions of amyl acetate was recorded at room temperature by a Renishaw Raman spectrometer equipped with a diffraction grating with a constant of 1200 lines/mm. An argon laser with a wavelength of 532 nm and a power of 50 mW was used to generate excitation light. The scattered light was recorded using a typical Renishaw CCD camera detector. FTIR spectra were obtained using an IRAffinity-1S Fourier spectrometer and managed with LabSolutions IR software.

3. Computational Method

All calculations are carried out in the Gaussian 09W program [27] using the DFT approach. The molecular structures of amyl acetate and ethanol are theoretically studied using the DFT/6-311++G(d, p) approach and the hybrid functional (Becke-3-Li-Yang-Parr) B3LYP [28, 29]. Spectra are drew using the Origin 8.5 software [30]. The geometric structure of the molecule is characterized using MEP methods [31]. The different analyses (AIM, RDG, ELF, and LOL) caried out using the MULTIWFN 3.8 bin (Win 64) and VMD program [32]. The hydrogen bond energy is calculated with the following formula:

$$E_{\text{int}} = E_{\text{complex}} - \sum_{i=1}^{n} E_i, \tag{1}$$

where E_{complex} is the energy of complex formation, $\sum_{i=1}^{n} E_i$ is the sum of energies of molecules participating in the complex formation.

4. Results and Discussion

4.1. Vibrational spectra of pure amyl acetate

Figure 1 shows the Raman and infrared spectra of amyl acetate. The figure indicates that the Raman spectra of pure amyl acetate are complicated, with many vibrational peaks. For example, the Raman spectrum of pure amyl acetate showed a frequency of 636 cm^{-1}, which was also seen at 634 cm^{-1} in the infrared absorption spectrum (FTIR) and 644 cm^{-1}

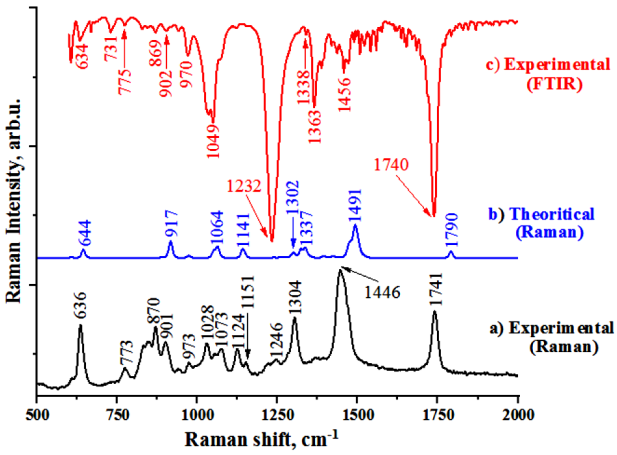

Fig. 1. Raman and FTIR spectra of amyl acetate

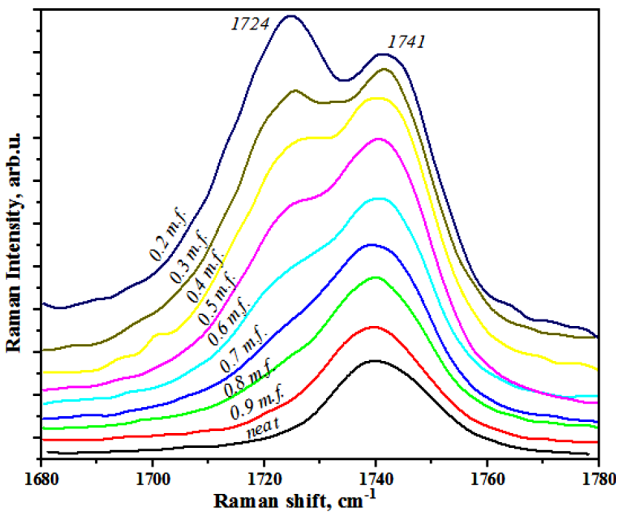

Fig. 2. Raman spectra of C=O stretching vibrational bands of amyl acetate-ethanol solution (in m.f. of amyl acetate)

at theoretically. In addition, the Raman spectrum revealed a spectral band corresponding to the C=O vibration at 1741 cm^{-1}, whereas the FTIR revealed the same band at 1740 cm^{-1}. In calculations, this band is equal to 1790 cm^{-1}. The experiments differed from the calculations because calculations, were performed for a single isolated gas molecule. In contrast, the experiments were performed on liquids, but the general pattern was maintained.

4.2. C=O vibrational bands of amyl acetate-ethanol solutions

Figure 2 illustrates the Raman spectra of amyl acetate-ethanol solution at various concentrations (0.9–0.2 mol fraction (m.f.)). The experimental results demonstrate that the C=O stretching vibration band of pure amyl acetate was detected at 1741 cm^{-1}. As the concentration of amyl acetate in the solution decreases, a new band at 1724 cm^{-1} emerges, as discussed below. The theory of resonance effect is often applied to explain the deformation of scattering spectra as concentrations increase in solutions. According to this theory, changes in Raman spectra during monomer association are induced by the splitting of their electronic energy states as a result of resonant interactions between the coupled molecules. Spectral changes of this sort can be observed, for example, during the combination of amyl acetate molecules with ethanolic solutions, as well as in combinations of polar solvents, such as alcohols, with a small ratio of the polar component of the substances. The deformation of the Raman spectra of amyl acetate in amyl acetate-ethanol mixture is shown as a function of the solution concentration (Fig. 2).

The scattering spectra are largely unchanged in the low concentration region (up to 0.8 m.f.) as bound molecules begin to form. As the concentration increases, the long-wave maxima of monomers decrease, while a new maximum develops and increases in the low-frequency part. This confirms the formation of associations. In this case, the spectral band of amyl acetate, or its monomers, appears at 1741 cm^{-1}. Due to hydrogen bonding, the spectral band corresponding to the C=O stretching vibration creates an additional band at 1724 cm^{-1} in amyl acetate-ethanol solution.

4.3. C=O vibrational bands of amyl acetate-heptane solutions

Because it is interesting to observe the C=O stretching vibration bands of Raman spectra involved in the intermolecular interaction of amyl acetate these bands were investigated. Figure 3 shows the C=O stretching vibrational bands of neat amyl acetate and its inert solution of heptane. The C=O vibrational band maximum in the neat state is 1741 cm^{-1}. As the concentration of amyl acetate decreases, the peak of the band shifts to higher frequencies. When concentration is 0.9 m.f. and 0.8 m.f., the peak of the C=O stretching vibration band is 1742 cm^{-1} and 1742 cm^{-1} respectively and these peaks are shifted to higher frequencies (1 and 2 cm^{-1}) compared to

the neat state. As the concentration of amyl acetate in the solution decreases, the frequency of the C=O stretching vibration band increases monotonically.

When the concentration of amyl acetate is 0.1 m.f, the band peak increases to 1750 cm^{-1} and shifts to a higher frequencies by 9 cm^{-1} compared to the neat state. One of the main reasons for the shift of the band maximum is intermolecular hydrogen H-bonding. That is, molecules of liquid amyl acetate bond to one another, and molecules of an inert solvent heptane begin to break these bonds. As the concentration of amyl acetate in the solution decreases, or as the concentration of heptane increases, the frequency of the C=O stretching vibration band shifts to higher frequencies, making the band simpler.

5. Molecular Electrostatic Potential (MEP) Surface

Amyl acetate has electrophilic points around the oxygen atom and nucleophilic points around the hydrogen atoms of the methyl and C–H groups. A neutral electrostatic potential exists between the hydrogen and carbon atoms of the CH_2 group of amyl acetate. The oxygen atom of the hydroxyl group in ethanol has a negative potential (red), while the hydrogen atom has a positive potential (blue). The electrostatic potential surfaces of amyl acetate-ethanol complexes change as molecules exchange charges. This confirms the existence of interactions between molecules.

Figure 4 shows the MEP surface for amyl acetate, ethanol, and amyl acetate-ethanol. According to studies, strong positive potentials surround the hydrogen atom in the C–H group, while strong negative potentials surround the oxygen atom in the ether carbonyl group. In addition, the other oxygen atom and the ether group have weak negative potentials. These results demonstrate that the hydrogen atom of the C–H group of amyl acetate and the hydrogen atom of the O–H group of ethanol can serve as electron acceptors, whereas the oxygen atoms in the ether group can act as electron donors. The oxygen atom of the C=O group donates more electrons than the oxygen atom of C–O. Amyl acetate is more likely to form a long chain through hydrogen bonding. When hydrogen bonds build between amyl acetate molecule clusters, molecules gain energy. Thus, in this work, the interaction of hydrogen bonds between amyl acetate-ethanol complexes was investigated.

5.1. Mulliken charge analysis

Mulliken atomic charge analysis is beneficial in explaining molecular behavior in complex systems. Because atomic charges control a variety of molecule characteristics such as electronic structure, reactivity, dipole moment, polarization, and vibrational spectrum [33]. Table 1 shows the Mulliken charge distribution of amyl acetate and its ethanolic complexes. Figure 5 shows the Mulliken charge distribution for these compounds. This distribution is essential for charge exchange between interacting molecules. All hydrogen atoms in amyl acetate and amyl acetate-1 ethanol complexes are positively charged, whereas oxygen atoms are negatively charged.

Due to the charge exchange between hydrogen and oxygen during the complex formation, the electron density on the carbon atom of C=O group increases notably. The atom of carbon charge changed from 0.262e to 0.266e (amyl acetate-1 ethanol) in the monomer. The electron density on the carbon atom of the C=O group increases significantly as a result of the charge exchange between hydrogen and oxygen during the complex formation. The charge of the carbon atom of the monomer changed from 0.262e to 0.266e (amyl acetate-1 ethanol). Similarly, the charge of the oxygen atom (O^2) changed from –0.276e to –0.291e of amyl acetate-1 ethanol (Table 1). The charge of the hydrogen (H^{32}) atom of ethanol increased from 0.296e to (amyl acetate-1 ethanol).

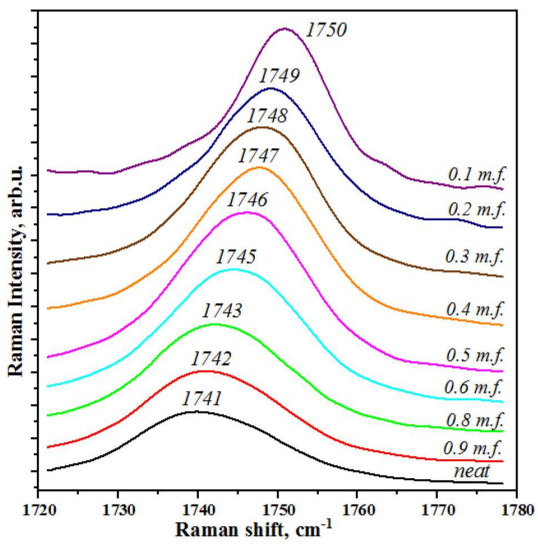

Fig. 3. Raman spectra of C=O stretching vibration bands of amyl acetate-heptane solution (in m.f. of amyl acetate)

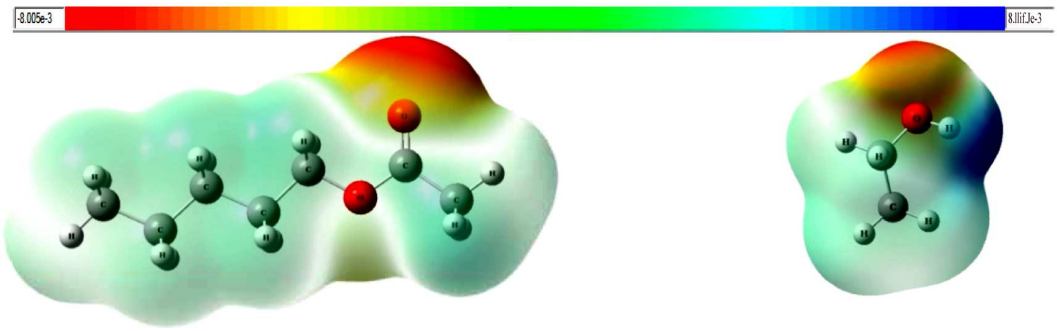

a *b*

Fig. 4. MEP surface of amyl acetate (*a*) and ethanol (*b*)

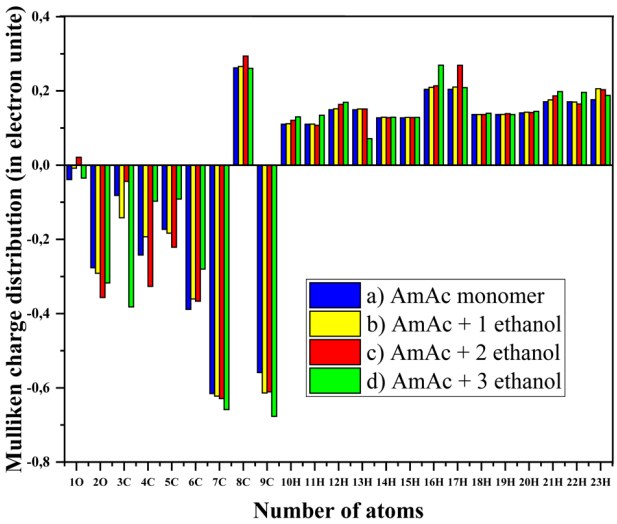

Fig. 5. Mulliken charge distribution of amyl acetate (AmAc)-ethanol complexes

These changes of charge distribution cause an increase of the bond length of the carboxyl group, leading to a change of frequencies at different solvent concentrations. When we look at the charge of the atoms participating in the amyl acetate-1 ethanol interaction, we can see that the charge modulus of C^8 and H^{21} has increased while C^3 and C^9 atomic charge modulus decreased. Figure 5 shows that the charge distribution for the amyl acetate-2 ethanol complex has also changed slightly, which is important for the atoms involved in the interaction.

5.2. Atoms in molecules (AIM) analysis

The AIM analysis was used to identify and estimate the energy of critical bond locations within amyl acetate-ethanol molecules. The Laplacian of electron density $\nabla^2\rho(r_c))$ and electron density $\rho(r_c)$ are the most commonly used approach for detecting interactions such as hydrogen bonds and identifying significant locations of their bindings [34, 35]. The bond

Mulliken charge distribution in amyl acetate (AmAc) molecule

Atomic number	Mulliken charge distribution (in electronic units)			
	Monomer	AmAc-1 ethanol	AmAc-2 ethanol	AmAc-3 ethanol
O^1	–0.038932	–0.008138	0.021296	–0.034710
O^2	–0.276401	–0.291422	–0.356474	–0.317529
C^3	–0.081432	–0.142028	–0.043990	–0.382039
C^4	–0.241971	–0.193266	–0.326431	–0.097270
C^5	–0.173080	–0.183496	–0.221292	–0.091539
C^6	–0.388542	–0.360629	–0.366746	-0.279931
C^7	–0.615446	–0.622304	–0.628925	-0.658512
C^8	0.262111	0.266064	0.293694	0.260813
C^9	–0.559034	–0.613742	–0.610652	-0.676842
H^{10}	0.110021	0.111376	0.120723	0.129869
H^{11}	0.110020	0.110521	0.107241	0.134358
H^{12}	0.149210	0.151523	0.163426	0.169365
H^{13}	0.149254	0.151360	0.151258	0.071388
H^{14}	0.127635	0.128927	0.127749	0.128847
H^{15}	0.127634	0.128510	0.128301	0.128578
H^{16}	0.204186	0.209551	0.213842	0.269345
H^{17}	0.204179	0.210237	0.269032	0.209082
H^{18}	0.136291	0.136470	0.136295	0.139575
H^{19}	0.136290	0.136753	0.138806	0.136480
H^{20}	0.140851	0.142497	0.141577	0.144942
H^{21}	0.170430	0.175790	0.186396	0.198207
H^{22}	0.170485	0.169827	0.164636	0.195998
H^{23}	0.176243	0.205800	0.203148	0.187755

lengths and bond energies of the hydrogen bonds were calculated for the investigated molecules. To find the probable intermolecular interactions between amyl acetate and ethanol were calculated with 1–3 complexes of ethanol and 1 amyl acetate. Amyl acetate and ethanol complexes may produce hydrogen bonds with the formula O–H...O=C.

Figure 6 shows the optimal geometry of amyl acetate-ethanol complexes. The amyl acetate and ethanol form closed-type hydrodimer complexes (Fig. 6, *a*). The dipole moment increased to 3.24D compared to the amyl acetate monomer. This is because amyl acetate and ethanol molecules are not symmetrical. The complex formation energy is 5.732 kcal/mol, and it is bonded by the two hydrogen bonds. The first is O–H...C=O between O^2 and H^{32} atoms (bond length 1.935 Å), second one is a weak bond (C–O...H(CH_3)) between O^{24} atom of ethanol and H^{23} atoms of amyl acetate (bond length 2.580 Å).

It was calculated by doubling the number of ethanol. In Figure 6, *b*, the H^{32} and H^{41} atoms of ethanol form a hydrogen bond with the O^2 atom of C=O group amyl acetate. The bond lengths are 1.969 Å and 2.009 Å, respectively, with a bond energy of 10.348 kcal/mol. The oxygen atoms in ethanol form a cyclic complex with CH_3 and C–H groups of amyl acetate through weak (bond length 2.562 and 2.447 Å) hydrogen bonds. In this way, calculations were carried out with the ethanol number increased by three (Fig. 6, *c*). The figure illustrates that the amyl acetate molecule creates strong hydrogen bonds with ethanol molecules through its two oxygens, whereas it forms weak hydrogen bonds through the carbon atoms of the methyl group. As the number of ethanol increases, the bond energies also increase.

5.3. Noncovalent interaction (NCI) and reduced density gradient (RDG) analysis of amyl acetate-ethanol complexes

The NCI index is used to describe intermolecular interactions and determine the nature of weak interactions. The NCI index is based on the RDG and gives additional information about noncovalent interactions [36–43]. NCI compares stabilizing and repulsive interactions at a certain point in space to determine the proportion of C=O...H hydrogen bonds [44, 45]. This analysis focused on the RDG, s function sign(λ_2)ρ, the multiple of electron density ρ, and

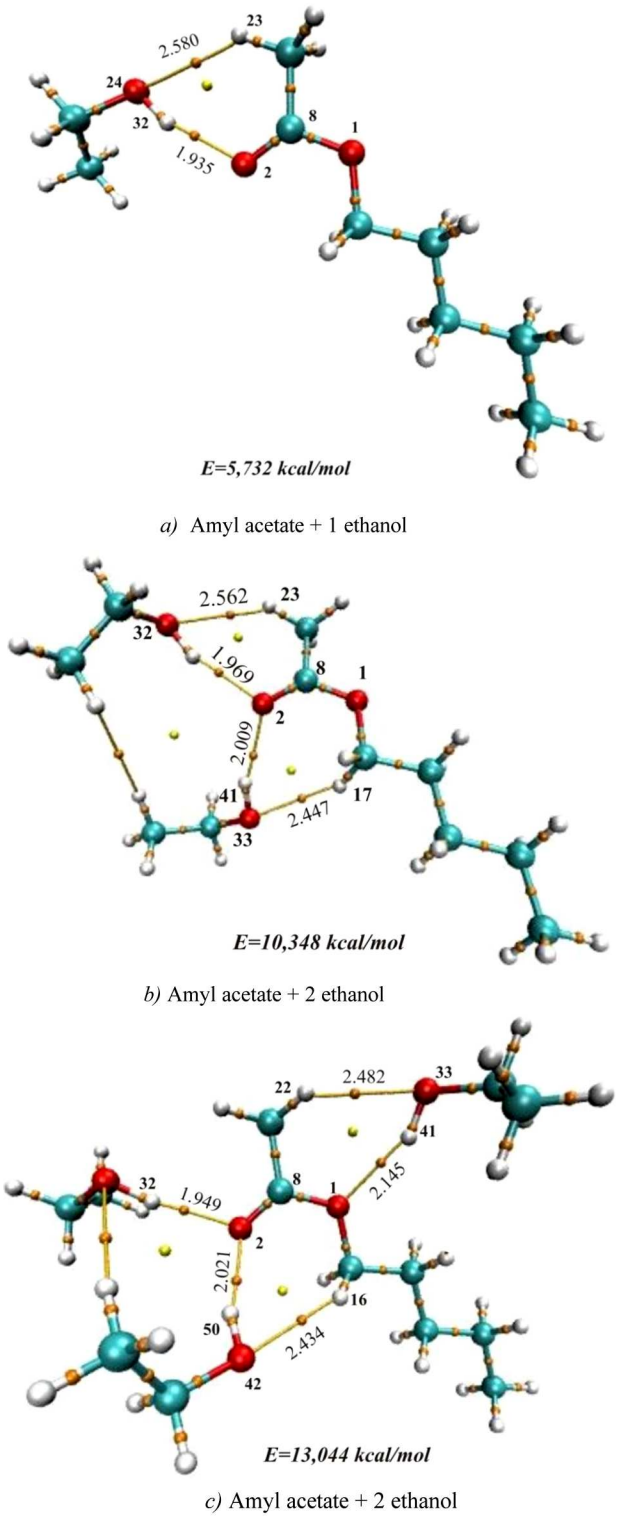

Fig. 6. Optimal geometry of amyl acetate-ethanol complexes

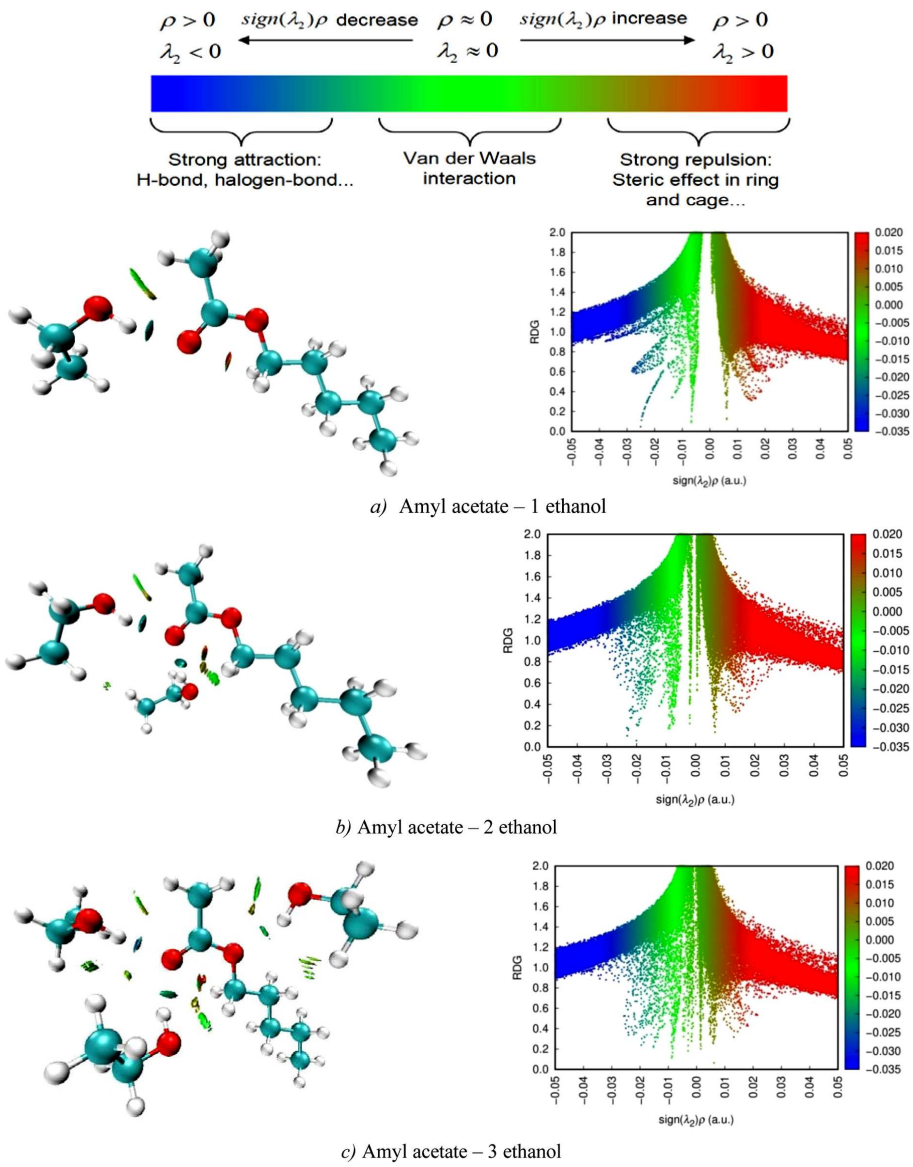

Fig. 7. NCI and RDG analysis for amyl acetate-ethanol complexes

the second eigenvalue of the electron density Hessian sign (λ_2)

$$S = \frac{1}{2(3\pi)^{1/3}} \frac{|\nabla\rho|}{\rho^{4/3}}. \quad (2)$$

Positive values of $\mathrm{sign}(\lambda_2)\rho$ indicate attraction, while negative values indicate stabilizing factors involving hydrogen bonding. Negative sign $(\lambda_2)\rho$ values show a strong bond. RDG analysis is used for comprehending the molecular structure of noncovalent interactions demonstrating strong attraction, strong repulsive, and neutral interactions with a reduced density gradient [46]. Image visualization based on electron density in the RDG parameter gives information about the nature of strong and weak interactions. In the RDG map, $\mathrm{sign}(\lambda_2)\rho$ indicates the difference between attraction and repulsion, whereas $\rho(\rho)$ represents the graph electron density [47]. When the sign $(\lambda_2)\rho$ is greater than 0, the RDG graph displays a red color range, indicating a strong steric effect. If

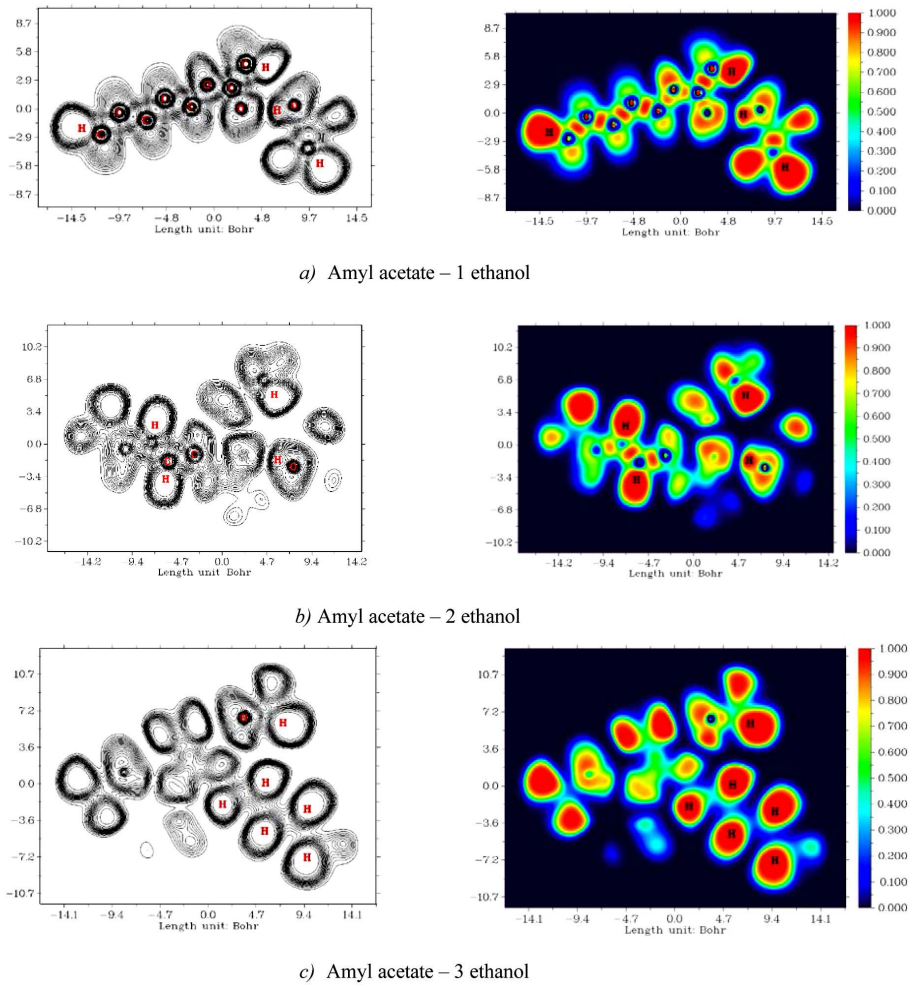

a) Amyl acetate – 1 ethanol

b) Amyl acetate – 2 ethanol

c) Amyl acetate – 3 ethanol

Fig. 8. ELF analysis for amyl acetate-ethanol complexes

sign(λ_2)ρ is less than 0, it indicates a strong attraction to dark green and blue colors. A value sign(λ_2)ρ near to 0 indicates the green color and Van der Waals interaction [48]. Figure 7 displays a 2D scatter plot and an RDG isograph. The red positively charged (0.02–0.05) sector on the RDG map represents a high repulsion and corresponds to the oxygen and methyl groups of amyl acetate (Fig. 4, *a*). The green color indicates that the negatively charged area (–0.01–0.01) has a weak interaction between the carbon of the methyl group of amyl acetate and the oxygen of the O–H group of ethanol, referred to as the Van der Waals interaction. The dark blue negatively charged sector (–0.02; –0.05) represents a strong H-bond in the form of O–H...O between the hydrogen of the O-H group of ethanol and the oxygen atom of the carbon group of amyl acetate. For the same reason, when the calculations are continued to include amyl acetate and three ethanol molecules, weak interactions between these molecules, referred to as van der Waals interactions, play an important role.

5.4. Electron localization function (ELF) and localized orbital locator (LOL) analysis for amyl acetate-ethanol complexes

The ELF and the LOL approaches can also be combined to investigate covalent bonding and electron density values [49]. These are the regions of the molecular area where each pair of electrons is most likely to be found [50]. Figures 8 and 9 show the color file projection map and contour map of ELF created by Multiwfn 3.8 program for amyl acetate-ethanol

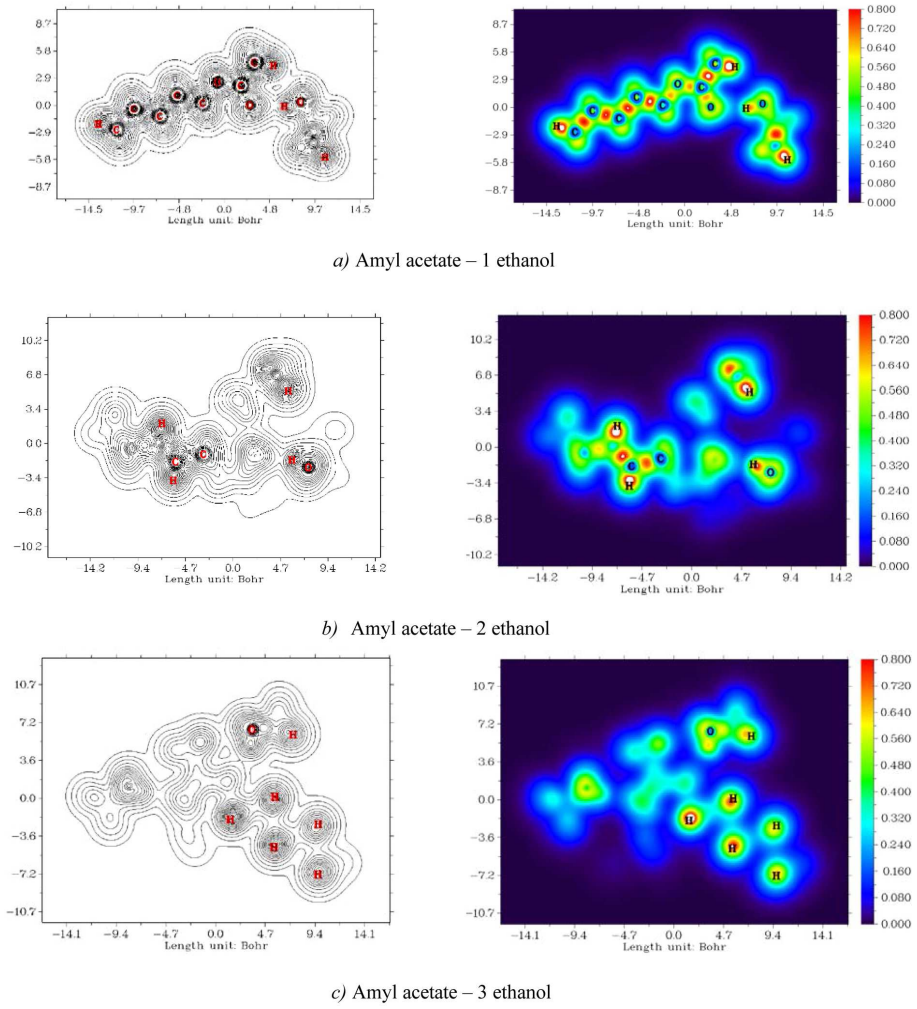

a) Amyl acetate – 1 ethanol

b) Amyl acetate – 2 ethanol

c) Amyl acetate – 3 ethanol

Fig. 9. LOL analysis for amyl acetate-ethanol complexes

molecules, respectively [51]. In general, ELF represents the electron pair density and scheme configuration on a scale of 0 to 1.0, including both bonded and nonbonded local electron pairs. A value less than 0.2 indicates that the electron field in the given molecule is delocalized. Similarly, LOL describes most of the localized orbital coverage, and the map surface occurs in the range from 0 to 1. In this situation, electron localization takes place at a specific location determined by electron density. Covalent bonds and lone electron pairs around hydrogen atoms have been identified to have the largest localization of bonded and non-bonded electron pairs for ELF and LOL. Because of their smaller values, the delocalization of ELE and LOL electron pairs was investigated in the structure of amyl acetate surrounding carbon atoms C^7, C^5, C^3, C^4, C_6, C^8, and C^9. In comparison, ELF provides more detailed and accurate information than LOL for the amyl acetate-ethanol complex.

5.5. Calculated C=O stretching vibrational bands of amyl acetate and ethanol complexes

Figure 10 illustrates the Raman spectrum of the C=O stretching vibration band of amyl acetate monomer and its complex with ethanol. The C=O stretching vibration peak for amyl acetate monomer is 1790 cm^{-1} (Fig. 10, *a*). In Fig. 10, *b*, the amyl acetate-1 ethanol dimer has a vibrational peak of 1759 cm^{-1}, which is 31 cm^{-1} lower than the frequency of monomer. Figure 10, *c* illustrates the C=O stretching vibration

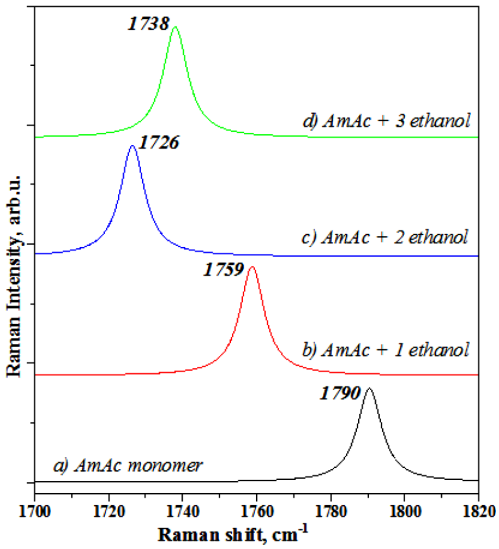

Fig. 10. Raman spectra of C=O stretching vibration band of amyl acetate (AmAc)-ethanol complexes

band (1726 cm^{-1}) of amyl acetate-2 ethanol complex, which, shifted to a lower frequency by 64 cm^{-1} as compared to the monomer. The low frequency shift is caused by the hydrogen atoms of both ethanols being bonded to the O^2 atom of C=O group of amyl acetate. When the ethanol number reaches three in the amyl acetate-ethanol complex, the peak of the C=O stretching vibration band equals 1738 cm^{-1} and shifts to a lower frequency of 52 cm^{-1} compared to the monomer. This is because the hydrogen atoms of two ethanols create a hydrogen bond through the O^2 atom of C=O group of amyl acetate, while the hydrogen atom of the third ethanol forms a hydrogen bond through the second O^1 atom of C–O–C group amyl acetate. So, as the number of ethanol molecules in the amyl acetate-ethanol complex increases, peak of the C=O vibration frequency decreases and shifts to a lower frequency. This corresponds to the hydrogen bond theory which stretching band shifting to a lower frequency [52].

6. Conclusion

The Raman and FTIR spectra of pure amyl acetate are complex due to the existence of complexes that have various depolarization coefficients in the liquid, and they are found to correlate to spectra obtained by quantum chemical calculations. The frequency of the C=O stretching vibration band of the amyl acetate molecule, which is involved in the hydrogen bonding, is determined experimentally to shift the vibration band at differed solvent concentrations. The C=O stretching vibration bands in the amyl acetate solution with an inert solvent heptane, are shown to shift to a higher frequencies. The experimental approach is used to investigate the solution of amyl acetate in ethanol at different concentrations (ranging from 0.9 to 0.2 m.f.). As the concentration of amyl acetate in the solution decreases, the long-wave peak (1741 cm^{-1}) of amyl acetate related to monomers decrease. However, a new peak appears and increases in its low-wavenumber part (1724 cm^{-1}), indicating that the O atom of the C=O group of the amyl acetate molecule forms a hydrogen bond as a form of C=O...H through the H atom of ethanol.

The mechanisms of molecular cluster formation of amyl acetate and its solution in ethanol are investigated using DFT and the B3LYP 6-311++G (d, p) bases set functions. When the number of ethanol molecules reaches three, the C=O vibrational band shifted to a lower frequency of 52 cm^{-1} than the monomer. This is due to the C=O...H hydrogen bond formed between amyl acetate and ethanol. For the same reason, the calculations showed that, among amyl acetate-ethanol molecules, weak interactions, i.e., van der Waals interactions, are dominant. Analysis of the Mulliken charge distribution of amyl acetate-ethanol, as well as different analyses (AIM, NCI, RDG, ELF, and LOL), provide information about the formation of hydrogen bonds between the molecules.

This work was financed by the Ministry of Higher Education, Science and Innovation of the Republic of Uzbekistan Foundation under project No. FZ-20200929385.

1. H. Hushvaktov, A. Jumabaev, I. Doroshenko, A. Absanov. Raman spectra and non-empirical calculations of dimethylformamide molecular clusters structure. *Vib. Spectrosc.* **117**, 103315 (2021).
2. A. Jumabaev, U. Holikulov, H. Hushvaktov, A. Absanov, L. Bulavin. Interaction of valine with water molecules: Raman and DFT study. *Ukr. J. Phys.* **67**, 602 (2022).
3. H.A. Hushvaktov, F.H. Tukhvatullin, A. Jumabaev, U.N. Tashkenbaev, A.A. Absanov, B.G. Hudoyberdiev, B. Kuyliev. Raman spectra and ab initio calculation of a structure of aqueous solutions of methanol. *J. Mol. Struct.* **1131**, 25 (2017).
4. F.H. Tukhvatullin, U.N. Tashkenbaev, A. Jumabaev, H. Hushvaktov, A. Absanov, G. Sharifov. Calculations and experimental studies of the aggregation of molecules of liq-

uid acetone by spectra of Raman scattering. *J. Nonlin. Opt. Phys. Mater.* **22**, 1350022 (2013).
5. F.H. Tukhvatullin, V.E. Pogorelov, A. Jumabaev, H.A. Hushvaktov, A.A. Absanov, A. Shaymanov. Aggregation of molecules in liquid methyl alcohol and its solutions: Raman spectra and ab initio calculations. *J. Mol. Struct.* **881**, 52 (2008).
6. S. Otajonov, S. Allaquliyeva, B. Eshchanov, N. Abdullayev, H. Eshkuvatov. Manifestation of the laws of vibrational motion of molecules of the condensed medium under the influence of laser radiation in the Raman spectrum. *Results in Optics* **13**, 100550 (2023).
7. S. Otajonov, B.X. Eshchanov, A.S. Isamatov. On possible models of thermal motion of molecules and temperature effect on relaxation of optical anisotropy in bromine benzene. *Ukr. J. Phys.* **56**, 1178 (2011).
8. B.A. Marekha, K. Sonoda, T. Uchida, T. Tokuda, A. Idrissi, T. Takamuku. ATR-IR spectroscopic observation on intermolecular interactions in mixtures of imidazolium-based ionic liquids $C_n$mimTFSA ($n = 2$–12) with DMSO. *J. Mol. Liq.* **232**, 431 (2017).
9. A. Jumabaev, H. Hushvaktov, B. Khudaykulov, A. Absanov, M. Onuk, I. Doroshenko, L. Bulavin. Formation of hydrogen bonds and vibrational processes in dimethyl sulfoxide and its aqueous solutions: Raman spectroscopy and Ab initio calculations. *Ukr. J. Phys.* **68**, 375 (2023).
10. G.A. Jeffrey. *An Introduction To Hydrogen Bonding* (Oxford university press, 1997) [ISBN: 978-0195095494].
11. L. Pauling. *The Nature of the Chemical Bond* (Cornell University Press, 1960) [ISBN: 978-0801403330].
12. J. Chocholoušová, V. Špirko, P. Hobza. First local minimum of the formic acid dimer exhibits simultaneously red-shifted O–H$\cdots$O and improper blue-shifted C–H$\cdots$O hydrogen bonds. *Phys. Chem. Chem. Phys.* **6**, 37 (2004).
13. O. Mishchuk, I. Doroshenko, V. Sablinskas, V. Balevicius. Temperature evolution of cluster structure in n-hexanol, isolated in Ar and N_2 matrices and in condensed states. *Struct. Chem.* **27**, 243 (2016).
14. Y. Tatamitani, B. Liu, J. Shimada, T. Ogata, P. Ottaviani, A. Maris, J.L. Alonso. Weak, improper, C–O...H–C hydrogen bonds in the dimethyl ether dimer. *J. Am. Chem. Soc.* **124**, 2739 (2002).
15. V. Balevicius, V. Sablinskas, I. Doroshenko, V. Pogorelov. Propanol clustering in argon matrix: 2D FTIR correlation spectroscopy. *Ukr. J. Phys.* **56**, 855 (2011).
16. H. Gasparetto, A.L.B. Nunes, F. de Castilhos, N.P.G. Salau. Soybean oil extraction using ethyl acetate and 1-butanol: From solvent selection to thermodynamic assessment. *J. Ind. Eng. Chem.* **113**, 450 (2022).
17. A. Oleinikova, L. Bulavin, V. Pipich. Critical anomaly of shear viscosity in a mixture with an ionic impurity. *Chem. Phys. Lett.* **278**, 121 (1997).
18. B.T.F. de Mello, I.J. Iwassa, R.P. Cuco, V.A. dos Santos Garcia, C. da Silva. Methyl acetate as solvent in pressurized liquid extraction of crambe seed oil. *J. Supercrit. Fluid.* **145**, 66 (2019).
19. L. Zhang, Y. Yang, Y. Li, J. Wu, S. Wu, X. Tan, Q. Hu. Highly efficient UV-visible-infrared photothermocatalytic removal of ethyl acetate over a nanocomposite of CeO_2 and Ce-doped manganese oxide. *Chin. J. Catal.* **43**, 379 (2022).
20. V.F. Korolovych, O.A. Grishina, O.A. Inozemtseva, A.V. Selifonov, D.N. Bratashov, S.G. Suchkov, L.A. Bulavin, O.E. Glukhova, G.B. Sukhorukov, D.A. Gorin. Impact of high-frequency ultrasound on nanocomposite microcapsules: In silico and in situ visualization. *Phys. Chem. Chem. Phys.* **18**, 2389 (2016).
21. A. Mahendraprabu, T. Sangeetha, P.P. Kannan, N.K. Karthick, A.C. Kumbharkhane, G. Arivazhagan. Hydrogen bond interactions of ethyl acetate with methyl Cellosolve: FTIR spectroscopic and dielectric relaxation studies. *J. Mol. Liq.* **301**, 112490 (2020).
22. Y. Zhou, Z. Wang, S. Gong, Z. Yu, X. Xu. Comparative study of hydrogen bonding interactions between N-methylacetamide and methyl acetate/ethyl formate. *J. Mol. Struct.* **1173**, 321 (2018).
23. H. Hushvaktov, B. Khudaykulov, A. Jumabaev, I. Doroshenko, A. Absanov, G. Murodov. Study of formamide molecular clusters by Raman spectroscopy and quantum-chemical calculations. *Mol. Cryst. Liq. Cryst.* **749**, 124 (2022).
24. R.M. Silverstein, F.X. Webster, D.J. Kiemle. *Spectrometric Identification of Organic Compounds* (Wiley, 1963) [ISBN: 978-0471791751].
25. O.W. Kolling. FTIR study of the solvent influence on the carbonyl absorption peak of ethyl acetate. *J. Phys. Chem.* **96**, 6217 (1992).
26. R. Sahana, P. Mounica, K. Ramya, G. Arivazhagan. Multimers of 1-propanol and their heteromolecular hydrogen bonds with ethyl acetate: Fourier transform infrared spectral studies. *J. Solut. Chem.* **52**, 1396 (2023).
27. M.J. Frisch *et al. Gaussian 09, Rev – D.1* (Gaussian Inc, Wallingford, 2009).
28. A.D. Becke. Density-funcitonal thermochemistry. III. The role of exact exchange. *J. Chem. Phys.* **98**, 5648 (1993).
29. C. Lee, W. Yang, R.G. Parr. Development of the Colle–Salvetti correlation energy formula into a functional of the electron density. *Phys. Rev. B* **37**, 785 (1998).
30. Origin Pro 8.5. OriginLab Coroporation, Northampton.
31. W. Humphrey, A. Dalke, K. Schulten. VMD: Visual molecular dynamics. *J. Mol. Graph.* **14**, 33 (1996).
32. T. Lu, F. Chen. Multiwfn: A multifunctional wavefunction analyzer. *J. Comput. Chem.* **33**, 580 (2012).
33. R.C. Dorca. Quantum mechanical basis for mulliken population analysis. *J. Math. Chem.* **36,** 231 (2004).
34. R. Bochicchio, R. Ponec, L. Lain, A. Torre. Pair population analysis within AIM theory. *J. Phys. Chem. A.* **104**, 9130 (2000).
35. B.A. Shainyan, N.N. Chipanina, T.N. Aksamentova, L.P. Oznobikhina, G.N. Rosentsveig, I.B. Rosentsveig. Intramolecular hydrogen bonds in the sulfonamide derivatives of oxamide, dithiooxamide, and biuret. FT-IR and DFT study, AIM and NBO analysis. *Tetrahedron* **66**, 8551 (2010).
36. W. Humphrey, A. Dalke, K. Schulten. VMD: Visual molecular dynamics. *J. Mol. Graph.* **14**, 33 (1996).

37. Th. Gomti Devi, Bhargab Borah. Non-coincidence effect study of NN-Dibutyl formamide in binary liquid mixtures. *J. Mol. Liq.* **309**, 113174 (2020).
38. Kh. Khushvaktov, A. Jumabaev, V. Pogorelov, U. Tashkenbaev, A. Absanov, G. Sharifov, B. Amrullaeva. Intermolecular hydrogen bond in acetic acid solutions. Raman spectra and ab initio calculations. *Am. J. Phys. Appl.* **6** (6), 169 (2019).
39. G. Pitsevich, I. Doroshenko, A. Malevich, E. Shalamberidze, V. Sapeshko, V. Pogorelov, L.G.M. Pettersson. Temperature dependence of the intensity of the vibration-rotational absorption band ν_2 of H_2O trapped in an argon matrix. *Spectrochim. Acta A.* **172**, 83 (2017).
40. R.F.W. Bader. A quantum theory of molecular structure and its applications. *Chem. Rev.* **91**, 893 (1991).
41. N. Chetry, Th. Gomti Devi. Intermolecular interaction study of l-threonine in polar aprotic solvent: Experimental and theoretical study. *J. Mol. Liq.* **338**, 116689 (2021).
42. Sh.S. Malaganvi, J.T. Yenagi, J. Tonannavar. Experimental, DFT dimeric modeling and AIM study of H-bond-mediated composite vibrational structure of Chelidonic acid. *Heliyon* **5** (5), e01586 (2019).
43. I. Rozas, I. Alkorta, J. Elguero. Behavior of ylides containing N, O, and C atoms as hydrogen bond acceptors. *J. Am. Chem. Soc.* **122** (45), 11154 (2000).
44. E.R. Johnson, S. Keinan, P. Mori-Sanchez, J. Contreras-Garcia, A.J. Cohen, W. Yang. *J. Am. Chem. Soc.* **132**, 6498 (2010).
45. J. Contreras-Garcia, E.R. Johnson, S. Keinan, R. Chaudret, J.-P. Piquemal, D.N. Beratan, W. Yang. *J. Chem. Theory Comput.* **7**, 625 (2011).
46. A. Demirpolat, F. Akman, A.S. Kazachenko. An experimental and theoretical study on essential oil of Aethionema sancakense: Characterization, molecular properties and RDG analysis. *Molecules*, **27**, 6129 (2022).
47. F. Akman, A. Demirpolat, A.S. Kazachenko, A.S. Kazachenko, N. Issaoui, O. Al-Dossary. Molecular structure, electronic properties, reactivity (ELF, LOL, and Fukui), and NCI-RDG studies of the binary mixture of water and essential oil of phlomis bruguieri. *Molecules.* **28**, 2684 (2023).
48. V.J. Reeda, V.B. Jothy, M. Asif, M. Nasibullah, N.S. Alharbi, G. Abbas, S. Muthu. Synthesis, solvent polarity (polar and nonpolar), structural and electronic properties with diverse solvents and biological studies of (E)-3-((3-chloro-4-fluorophenyl) imino) indolin-2-one. *J. Mol. Liq.* **380**, 121709 (2023).
49. Savithiri Sambandam, Bharanidharan Sarangapani, Sugumar Paramasivam, Rajeevgandhi Chinnaiyan. Molecular structure, vibrational spectral investigations (FT-IR and FT-Raman), NLO, NBO, HOMO-LUMO, MEP analysis of (E)-2-(3-pentyl-2,6- diphenylpiperidin-4- ylidene)-N phenylhydrazinecarbothioamide based on DFT and molecular docking studies. *Biointerface Res. Appl. Chem.* **11**, 11833 (2021).
50. K. Arulaabaranam, S. Muthu, G. Mani, A.S. Ben Geoffrey. Speculative assessment, molecular composition, PDOS, topology exploration (ELF, LOL, RDG), ligand-protein interactions, on 5-bromo-3 nitropyridine-2-carbonitrile. *Heliyon.* **7**, e07061 (2021).
51. M. Lawrence, E. Isac Paulraj, P. Rajesh. Spectroscopic characterization, electronic transitions and pharmacodynamic analysis of 1-phenyl-1,3-butanedione: An effective agent for antipsychotic activity. *Chem. Phys. Impact.* **6**, 100226 (2023).
52. A. Jumabaev, B. Khudaykulov, I. Doroshenko, H. Hushvaktov, A. Absanov. Raman and *ab initio* study of intermolecular interactions in aniline. *Vib. Spectrosc.* **122**, 103422 (2022).

Received 14.05.24

А. Жумабаєв, Х. Хушвактов, А. Абсанов,
Б. Худайкулов, З. Ерназаров, Л. Булавін

КОЛИВАЛЬНІ СПЕКТРИ ТА КОМП'ЮТЕРНЕ МОДЕЛЮВАННЯ АМІЛАЦЕТАТУ: MEP, AIM, RDG, NCI, ELF ТА LOL МЕТОДИ АНАЛІЗУ

Робота присвячена дослідженню біологічно активного чистого амілацетату та його розчинів в етанолі та гептані. Згідно з результатами експерименту, при зниженні концентрації амілацетату в спектрі розчину амілацетату в етанолі з'являється додаткова смуга з боку низьких частот. Основною причиною утворення такої додаткової смуги є міжмолекулярний водневий зв'язок між амілацетатом і етанолом. У розчині амілацетату в гептані спектральна смуга, що відповідає валентним C=O коливанням, зміщується в бік вищих частот із зменшенням концентрації амілацетату в розчині. Це пояснюється тим, що гептан порушує міжмолекулярні взаємодії в розчині, що приводить до більш простої спектральної смуги, яка відповідає валентному коливанню C=O. Розрахунками також досліджено взаємодії в комплексах амілацетат-етанолу та їх спектральні прояви. Виявилося, що енергія утворення комплексу зростає зі збільшенням числа молекул, але середня енергія водневого зв'язку, яка припадає на один зв'язок, залишається незмінною. Метод теорії функціонала густини (density functional theory, DFT) був використаний для аналізу низки структурних параметрів: розподілу зарядів атомів за Маллікеном, термодинамічних параметрів, поверхні молекулярного електростатичного потенціалу (molecular electrostatic potential, MEP) та розподілу атомів у молекулах (atoms in molecules, AIM). Було також проведено аналіз деяких квантово-хімічних параметрів, як-от: аналіз редукованого градієнта густини (reduced density gradient, RDG) і нековалентної взаємодії (noncovalent interaction, NCI), аналіз функцій локалізації електронів (electron localization functions, ELF) та аналіз локалізованого орбітального локатора (localized orbital locator, LOL).

Ключові слова: раманівська спектроскопія, квантово-хімічні розрахунки, теорія функціонала густини, водневий зв'язок, молекулярний електростатичний потенціал, функція локалізації електронів, локалізований орбітальний локатор, RDG діаграма, розподіл заряду за Маллікеном, амілацетат, етанол, гептан.